frontiers | Frontiers in Marine Science

TYPE Original Research
PUBLISHED 11 March 2025
DOI 10.3389/fmars.2025.1518631

OPEN ACCESS

EDITED BY
Martin F. Soto-Jimenez,
National Autonomous University of Mexico, Mexico

REVIEWED BY
Peng Zhang,
Guangdong Ocean University, China
Takahito Ikenoue,
Japan Agency for Marine-Earth Science and Technology (JAMSTEC), Japan
Duminda Senevirathna,
Uva Wellassa University, Sri Lanka

*CORRESPONDENCE
Yangjun Chen
yj-chen@jou.edu.cn

RECEIVED 28 October 2024
ACCEPTED 24 February 2025
PUBLISHED 11 March 2025

CITATION
Chen Y, Zhang X, Yang Y and Chen M (2025) Natural abundance isotope techniques offer a key to better deciphering the impact of microplastics on the nitrogen cycle.
Front. Mar. Sci. 12:1518631.
doi: 10.3389/fmars.2025.1518631

Natural abundance isotope techniques offer a key to better deciphering the impact of microplastics on the nitrogen cycle

Yangjun Chen [1,2,3]*, Xingzhou Zhang[1], Yuanyuan Yang[1] and Min Chen[4]

[1]School of Marine Science and Fisheries, Jiangsu Ocean University, Lianyungang, China, [2]Co-Innovation Center of Jiangsu Marine Bio-industry Technology, Jiangsu Ocean University, Lianyungang, China, [3]Jiangsu Key Laboratory of Marine Biotechnology, Jiangsu Ocean University, Lianyungang, China, [4]College of Ocean and Earth Sciences, Xiamen University, Xiamen, China

As human activities intensify, ecosystems are constantly being polluted by microplastics, which may change the microbe-driven nitrogen cycling and associated nitrous oxide emissions therein. However, the exact impact of microplastics on specific nitrogen cycling processes remains to be clarified, limiting accurate assessments of nitrous oxide production. Additionally, a gap in our understanding of the isotopic dynamics of nitrogen cycling under the impact of microplastics restricts deeper insights into nitrogen cycling in microplastic-polluted environments. Accordingly, this study represents the first integration of natural abundance isotope techniques with microcosm experiments involving various microplastics, offering a novel approach for detailed investigation into the impacts of microplastics on the nitrogen cycle dynamics and their potential role in regulating nitrous oxide production. Our results suggest that microplastics of different sizes (0.02 mm, 0.1 mm, and 1 mm) and polymer types (polypropylene, polyvinyl chloride, polyamide, and polyethylene) impact both nitrite production and consumption, highlighting the important role of size in these processes. Particularly, nitrite dual isotopic signatures help identify specific nitrogen cycling processes impacted by microplastics. More importantly, isotopic evidence indicates that nitrite may be lost from the environment primarily by reduction to gaseous products nitrous oxide or dinitrogen in polyethylene and polyvinyl chloride, especially the largest-size polyamide treatments. Conversely, polypropylene treatment, especially at large sizes, may promote nitrite oxidation, thus retaining more nitrogen within the environment. Our findings offer a new paradigm for the comprehensive assessment of the impact of microplastics on the nitrogen cycle and highlight the importance of considering microplastics when assessing greenhouse gas emissions, especially in the context of increasing microplastic pollution.

KEYWORDS

microplastics pollution, nitrite cycle, nitrous oxide, isotopic dynamics, climate change

1 Introduction

Nitrite (NO_2^-) is a key intermediate in the nitrogen (N) cycle, which is involved in almost all N biogeochemical processes driven by microbes. Its main fate in the environment, being reduced via denitrification and anaerobic ammonium oxidation (anammox) or oxidized through NO_2^- oxidation, directly affects the reconciliation of the bioavailable N budget and the production of the greenhouse gas nitrous oxide (N_2O) (Zhang et al., 2020). However, ecosystems have changed in recent decades due to human activities (e.g., environmental pollution), and the microbe-driven N cycle may also change accordingly (Fang et al., 2024; Greenfield et al., 2022; Hu et al., 2023; Li et al., 2020; Lyu et al., 2024; Seeley et al., 2020; Wang et al., 2024; Yu et al., 2022; Zhu et al., 2022), which necessitates a continuous updating of our knowledge of NO_2^- cycle and its associated production of N_2O in a changing environment.

Microplastics (MPs, generally defined as tiny plastic fragments or particles with a diameter of <5 mm; Hartmann, 2019), an emerging environmental pollutant, are found in various ecosystems in different shapes, sizes, ages, and polymer types (Cluzard et al., 2015; de Souza MaChado et al., 2019; Song et al., 2023; Wang et al., 2023), and have an impact on the cycling of elements therein (Fang et al., 2024; Green et al., 2016; Greenfield et al., 2022; Hu et al., 2023; Hope et al., 2020; Li and Liu, 2022; Lyu et al., 2024; Rillig et al., 2021; Riveros et al., 2022; Seeley et al., 2020; Sun et al., 2023; Yin et al., 2023; Wang et al., 2024; Zhu et al., 2022). Sediment represents the ultimate sink for MPs in marine water (Lebreton et al., 2017) because MPs will continue to be deposited, albeit over a longer period of time. Since sediment is a hotspot for microbial activity, these settled MPs may have an impact on microbially mediated elemental cycling in the sediment, such as the N cycle (Chen et al., 2022a; Fang et al., 2024; Green et al., 2016; Hope et al., 2020; Lyu et al., 2024; Seeley et al., 2020) and carbon cycle (Ikenoue et al., 2024). This impact is now considered to stem from the formation of biofilms on the surface of MPs (Amaral-Zettler et al., 2020; Oberbeckmann et al., 2015; Pinnell and Turner, 2019; Su et al., 2022); the adsorption of other pollutants, nutrients, and organic matter by MPs (Ikenoue et al., 2022; Mato et al., 2001; Wang et al., 2020); the modification of the physicochemical properties of the sediment by MPs (Cluzard et al., 2015; de Souza MaChado et al., 2019; Fang et al., 2024; Wan et al., 2018; Zhang et al., 2019); and the release of MP additives (Azizi et al., 2021; Seeley et al., 2020; Vo and Pham, 2021). Based on these, MPs directly or indirectly impact the key microbes (e.g., nitrifiers, denitrifiers, and anammox bacteria), enzymes [e.g., ammonia monooxygenase, nitrate (NO_3^-) reductase, and NO_2^- reductase] and functional genes (e.g., *amoA*, *nirS*, and *nirK*) that regulate N transformation, and consequently the N cycling process (e.g., nitrification, denitrification, and anammox).

However, the exact impact of MPs on specific N cycle processes remains uncertain, limiting the accurate estimation of N_2O production linked to these processes (Wang et al., 2024). In addition, there is still a gap in the understanding of the isotopic dynamics of the N cycle under MP pollution, limiting the in-depth understanding of the N cycle in modern MP-polluted environments. The natural abundance stable isotope techniques may be able to address these issues, as the N cycle is composed of various N transformations driven by diverse microbes that operate to give unique isotopic signatures to N species (Buchwald and Casciotti, 2013; Casciotti, 2016a, 2016b; Chen et al., 2021, Chen et al., 2022a; Chen and Chen, 2022). These isotopic signatures can trace the sources, transformations, internal cycles, and losses of N (Buchwald and Casciotti, 2013; Casciotti, 2016a, 2016b; Chen et al., 2021, 2022; Chen and Chen, 2022). However, this approach is not yet in the field, leaving an unanswered question regarding the potential impact of MPs on the N and oxygen (O) isotope dynamics in the N cycle. Furthermore, the impact of MP size on N cycling has not yet been well discussed. This is obviously an issue that needs to be addressed (Lee et al., 2022; Li and Liu, 2022; Wang et al., 2024) because changes in MP size can impact their own physical disturbance, adsorption, and biofilm formation, which may have an impact on N cycling processes (Amaral-Zettler et al., 2020; Cluzard et al., 2015; de Souza MaChado et al., 2019; Oberbeckmann et al., 2015; Pinnell and Turner, 2019; Su et al., 2022; Wan et al., 2018; Wang et al., 2020; Zhang et al., 2019). Taken together, we have gradually recognized the impact of MPs on the N cycle (Chen et al., 2022b; Fang et al., 2024; Greenfield et al., 2022; Hu et al., 2023; Li et al., 2020; Lyu et al., 2024; Seeley et al., 2020; Wang et al., 2024; Yu et al., 2022; Zhu et al., 2022), but an accurate understanding of the N cycle under MP pollution remains elusive due to the above-mentioned knowledge gaps.

The natural abundance of N [$\delta^{15}N_{NO2} = (^{15}N/^{14}N_{Sample}/^{15}N/^{14}N_{Air} - 1) \times 1000‰$] and O [$\delta^{18}O_{NO2} = (^{18}O/^{16}O_{Sample}/^{18}O/^{16}O_{VSMOW} - 1) \times 1000$ ‰] isotope ratios of NO_2^- are ideal tools for probing the NO_2^- cycle (Buchwald and Casciotti, 2013; Casciotti, 2016a, 2016b; Chen et al., 2021; Chen et al., 2022a; Chen and Chen, 2022). Accordingly, with the aid of this tool, MPs of different sizes (0.02 mm, 0.1 mm, and 1 mm) and polymer types [polypropylene (PP), polyvinyl chloride (PVC), polyamide (PA), and polyethylene (PE)] were deployed to provide detailed information on NO_2^- cycling in the context of MP pollution (Supplementary Figure S1).

2 Materials and methods

2.1 Sampling stations and microcosm experimental design

Sediment samples were collected in July 2023 from the coastal intertidal zone of Haizhou Bay, Western Yellow Sea, China, following low tide, and simultaneously, ambient seawater was also collected at the same site. The sediments were sieved on-site to remove larger impurities and macroorganisms, and subsequently dried in air and sieved through a 2mm stainless steel mesh to achieve complete homogenization and removal of small impurities and interstitial water (Seeley et al., 2020). Concurrently, ambient seawater was filtered on-site using a 0.45 μm Millipore membrane prior to use.

The microcosm experimental design includes four commonly used MP treatments (PP, PVC, PA, and PE, reviewed in Wang et al.,

2024) and a no MP control treatment, with replicates per treatment (Supplementary Figure S1). These MPs are commercially available (Shenzhen Guangyuan Plasticisation Co., Ltd., China; high purity, greater than 99%) and are made in specific sizes as per the requirements of our experiments. MPs of different polymer types were further treated at different sizes (0.02 mm, 0.1 mm, and 1 mm; n = 26; Supplementary Figure S1). It needs to be clarified that the specific size of the MPs selected may not be fully representative of the size characteristics of MPs in diverse sediments, but rather reflect the range of sizes in which MPs may be present in environmental sediments (reviewed in Wang et al., 2024). The choice of these MPs was based on the main types of MPs commonly observed in the water column at the location where the sediment samples were collected (Song et al., 2023), in order to ensure a realistic representation of actual conditions. Furthermore, these are also the types of MPs that are frequently selected in other studies (reviewed in Wang et al., 2024), thus enabling a meaningful comparison. A relatively practical concentration of MPs (0.5% w/w) was set for the experiment based on available studies (Baysal et al., 2020; Fang et al., 2024; Seeley et al., 2020; Wang et al., 2024). We weighed 300 grams of the above fully homogenized sediment into a 1L beaker (sediment sample depth of 3 cm) and added the different polymer types and sizes of MPs mentioned above to achieve a consistent concentration (weight ratio to wet sediment), followed by seawater addition without disturbing the sediment as much as possible (Seeley et al., 2020). Prior to the start of the incubation experiment, the microcosm was gently aerated to maintain oxygen in the overlying water and to allow an oxic/anoxic gradient to develop in the sediment over a 24-hour period (Seeley et al., 2020). The control treatment followed the same steps as the MP treatment except that no MPs were added. Subsequently, the experiments were operated at room temperature (20°C), and each beaker was covered with a piece of tin foil for the duration of the experiments to prevent water evaporation or other disturbances caused by other factors.

The overlying water samples were collected at 30 mL on days 1, 3, 7, 18, and 25 of the experimental system. For NO_2^- concentration analysis, the samples were measured immediately or frozen for later measurement. For NO_2^- dual isotope analysis, 6 M sodium hydroxide was added to preserve the samples (prevent O isotope exchange between NO_2^- and H_2O) for isotopic measurement (Casciotti et al., 2007; Chen et al., 2021, 2022; Chen and Chen, 2022).

2.2 Concentration and isotope measurements

NO_2^- concentration was determined on a QuAAtro flow analyzer (Seal, Germany) by the flow injection technique using a Greiss-Ilosvay colorimetric method (Strickland and Parsons, 1972), with steps including reagent preparation (sulfanilamide and N-(1-naphthyl) ethylenediamine), and correction of blanks and refractive index.

The $\delta^{15}N_{NO2}$ and $\delta^{18}O_{NO2}$ were determined using the well-established azide reduction method (McIlvin and Altabet, 2005). Depending on the NO_2^- concentration, an appropriate sample volume (calculated based on an optimal injection size of 20 nmol for N_2O formed by the sample) was pipetted into a pre-acid washed and scorched 20 mL headspace vial. The vial was then sealed with an aluminum cap and silica pad, and purged with helium to remove any N_2O present (Chen et al., 2021; Chen et al., 2022a; Chen and Chen, 2022). The reaction reagents in the azide reduction method include sodium azide and acetic acid solutions, which were prepared and used on the same day. These solutions were added to a 50 mL headspace vial in a 1:1 ratio (the volume added is determined by the number of samples) and purged with helium for half an hour (Chen et al., 2021; Chen et al., 2022a; Chen and Chen, 2022). Since the sample had a high pH with the addition of sodium hydroxide, the concentration of the acetic acid solution needed to be increased to 7.84 M in order to achieve the conditions for optimal reaction rate (pH = 4.5, Chen et al., 2021; Chen et al., 2022a; Chen and Chen, 2022; Hu et al., 2016). After purging, 0.9 mL of sodium azide-acetic acid buffer solution was transferred to the sample vial with a syringe for reaction, and the reaction was ended by adding 0.5 mL of 10 M sodium hydroxide at 1 hour (Chen et al., 2021; Chen et al., 2022a; Chen and Chen, 2022). The N_2O produced by the reaction was automatically extracted, purified, concentrated, and analyzed online using a Thermo Finnigan Gasbench II purge-trap system interfaced with a DELTAplus XP isotope ratio mass spectrometer. To calibrate the isotope values of the samples, the NO_2^- isotopic standards (RSIL-N23, RSIL-N7373, and RSIL-N10219, Casciotti et al., 2007) were preserved and processed in the same procedure as the samples. A set of reference standards was inserted every 6–10 samples for analysis. The volume of the reaction solution was kept the same for each sample and standard to minimize the effect of pH in the azide reduction reaction (Granger et al., 2020; Kobayashi et al., 2021). The N content of the standards was matched to the samples to minimize the effect of sample size on the isotopic analysis (Granger et al., 2020; Kobayashi et al., 2021). The mean standard deviations for all replicate measurements of samples and standards in this study were 0.6‰ for $\delta^{15}N$ and 0.4‰ for $\delta^{18}O$, respectively.

3 Results and discussion

3.1 Regulation of the nitrite pool by MPs

3.1.1 Nitrite accumulation stage

We found distinct changes in NO_2^- concentration at different incubation times (Figure 1). On day 18 of the incubation experiment, there was a significant increase in the NO_2^- concentration in both control and MP treatments compared to the initial and day 7 (Figure 1), with the highest NO_2^- concentration of 51.24 ± 5.09 μmol L^{-1} recorded in the PP-1mm treatment (Figure 1A). Therefore, this period belongs to the NO_2^- accumulation stage, which is similar to the previous results (Seeley et al., 2020; Zhu et al., 2022). Although the NO_2^- concentration increased in each treatment compared to the initial and day 7, differences were observed between the control and MP

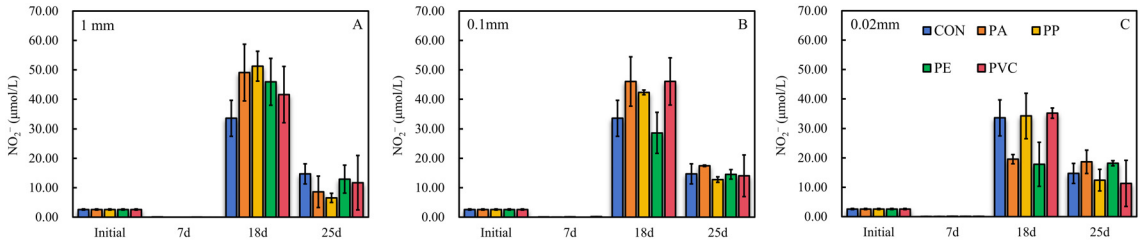

FIGURE 1
Changes in nitrite concentration during the incubation experiment. **(A)** represents the case of MP treatments of different polymer type at the 1 mm setting and the control (CON, no MPs in the sediment), while **(B, C)** are the scenarios at the 0.02 mm and 0.1 mm settings, respectively. The black lines are error bars (n = 2 per treatment).

sediments, and between the MP treatments with different polymer types and sizes (Figure 1). The difference in NO_2^- accumulation concentration between the control and the MP treatments depended on the polymer type of the MPs, which either negatively or positively impacted NO_2^- accumulation (Figure 1), supporting the previously proposed role of MP polymer type in regulating N transformation (reviewed in Wang et al., 2024). Notably, our results clearly identify the role of MP size in NO_2^- production (Figure 2). Interestingly, the degree of NO_2^- accumulation increased with increasing size in the PA treatment (Figure 2), with the concentration being progressively higher than in the control. In particular, the greatest increase in NO_2^- concentration was found when the size changed from 0.02 to 0.1 mm (Figures 1B, C and 2). Similar scenarios were also observed in the PE, PVC, and PP treatments (Figures 1, 2).

The accumulation of NO_2^- may involve processes such as ammonia (NH_3) oxidation, assimilatory NO_3^- reduction, and dissimilatory NO_3^- reduction (Buchwald and Casciotti, 2013; Casciotti, 2016a, 2016b; Chen et al., 2021; Chen et al., 2022a; Chen and Chen, 2022). Although assimilatory NO_3^- reduction is also responsible for NO_2^- production, this process was not considered in our microcosm due to the absence of phytoplankton. Thus, the different polymer types and sizes of MPs in this study have different impacts on the degree of NO_2^- accumulation, implying that MP treatments with higher (or lower) NO_2^- concentrations may promote (or impede) NO_2^- production, NH_3 oxidation, or dissimilatory NO_3^- reduction, as compared to the control (See further isotopic analyses below).

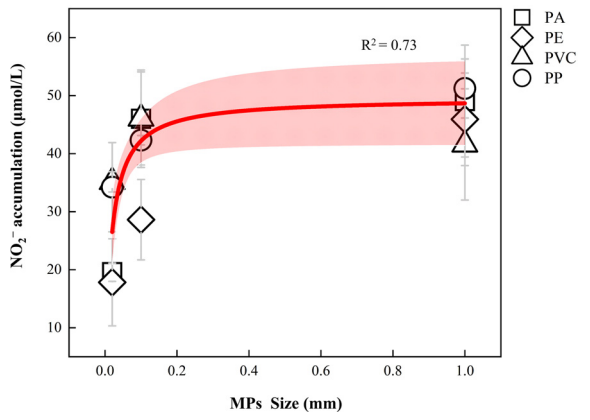

FIGURE 2
The impact of MP size on nitrite production during the nitrite accumulation stage. The red shading shows the 95% confidence intervals and grey lines are error bars.

3.1.2 Nitrite consumption stage

Upon reaching day 25, the NO_2^- concentration in each treatment showed a declining trend in comparison to day 18 (Figure 1), with the PP-1mm treatment showing the greatest decline, suggesting that this stage was characterized by the consumption of NO_2^-. Similar to the previous stage, the size and polymer type of MPs also played different roles in NO_2^- consumption (Figure 1). As the size increased, the degree of decrease in NO_2^- concentration in the PA, PE, PVC, and PP treatments all showed an increasing trend (Supplementary Figure S2) and were greater than that of the control. Furthermore, the greatest decrease in NO_2^- concentration was also recorded when the size varied between 0.02 mm and 0.1 mm (Supplementary Figure S2), which aligns with the characteristics of the previous stage (Figure 2). At a fixed size, we also observed a variation in NO_2^- consumption with the different polymer types of the MPs.

The decrease in NO_2^- concentration during this stage was due to the operation of NO_2^--consuming processes including the oxidation of NO_2^- to NO_3^- through the process of NO_2^- oxidation and the reduction of NO_2^- to gaseous products N_2O or dinitrogen (N_2) through the process of denitrification (dissimilatory NO_2^- reduction) or anammox (Buchwald and Casciotti, 2013; Casciotti, 2016a, 2016b; Chen et al., 2021; Chen et al., 2022a; Chen and Chen, 2022). Although the assimilation of NO_2^- by phytoplankton is also a NO_2^--consuming process (Buchwald and Casciotti, 2013; Casciotti, 2016a, 2016b; Chen et al., 2021; Chen et al., 2022a; Chen and Chen, 2022), it was excluded from consideration in the same way that assimilatory NO_3^- reduction was not considered. Thus, the difference in NO_2^- consumption under different polymer types and sizes of MP treatments as compared to the control may be due to the regulatory impact of these MP treatments on NO_2^- oxidation, dissimilatory NO_2^- reduction, or anammox.

Our results clearly show that NO_2^- production and consumption vary with MP polymer type and size, among which the impact of MP size deserves special attention (Figure 2 and Supplementary Figure S2). The variation in sediment response to different MPs may be attributed to the diverse physicochemical properties of polymers and their associated additives, and the biofilm formation on MP surfaces (Amaral-Zettler et al., 2020; Azizi et al., 2021; Oberbeckmann et al., 2015; Pinnell and Turner, 2019; Seeley et al., 2020; Su et al., 2022; Vo and Pham, 2021). These factors can differentially influence microbial activity, enzyme functions, and functional genes related to the N cycle, thereby altering biogeochemical processes within sediment ecosystems (Wang et al., 2024; Seeley et al., 2020; Shen et al., 2022; Su et al., 2022). In particular, the formation of biofilms on MPs in aquatic environments facilitates microbial adhesion and enhances local nutrient availability, leading to shifts in microbial community composition and activity, which in turn modulate N transformation processes (Wang et al., 2024; Seeley et al., 2020; Shen et al., 2022; Su et al., 2022). Moreover, the interactions between biofilms and MPs play a pivotal role in N cycling, as biofilm structures create microhabitats that influence microbial metabolic pathways and stress responses, particularly under environmental perturbations (Shen et al., 2022). These microhabitats can serve as hotspots for N transformations, creating conditions that either promote or impede key microbial processes such as nitrification and denitrification (Wang et al., 2024; Seeley et al., 2020; Shen et al., 2022; Su et al., 2022). Thus, the interplay between MP characteristics, biofilm development, and microbial dynamics is crucial in shaping N cycling within sedimentary environments.

Furthermore, the MP-size-dependent variation may be related to changes in their surface area, which influence biofilm formation and microbial colonization (Amaral-Zettler et al., 2020; Lebreton et al., 2017; Oberbeckmann et al., 2015; Su et al., 2022). Additionally, MPs significantly alter sediment properties, including porosity, pH, and oxygen availability (Cluzard et al., 2015; de Souza MaChado et al., 2019, 2019; Fang et al., 2024), thereby impacting microbial communities involved in N cycling. A notable effect of MPs in sediment ecosystems is their ability to increase porosity, which may enhance oxygen diffusion (Cluzard et al., 2015) and subsequently promote aerobic microbial processes such as nitrification. This mechanistic pathway aligns with our observations that the accumulation of NO_2^- exhibited a positive correlation with increasing MP size (Figure 2). However, it is important to recognize that once oxygen flux reaches a threshold sufficient to sustain nitrification, any further increase in MP size may have a diminishing impact on NO_2^- accumulation (Figure 2). This suggests a potential saturation effect, where oxygen availability ceases to be a limiting factor beyond a certain MP size. In our experimental conditions, the medium MP size likely provided adequate oxygen flux to support nitrification, which could explain why the increase in NO_2^- accumulation at the largest MP size was not significantly higher than at the medium MP size (Figure 2). This suggests that while MP size variation can initially enhance NO_2^- production, the incremental benefits diminish as size increases beyond a certain threshold. The identified role of MP size on NO_2^- production and consumption may help to explain the inconsistent findings regarding the impact of MPs on the N transformation process proposed in different studies (3). For example, the impact of PE on the N transformation process may be either positive or negative in different studies (Dai et al., 2020; Fang et al., 2024; Li et al., 2020; Seeley et al., 2020; Yin et al., 2023). Such disparate roles are also identified in our study, where PE, for instance, showed a positive or negative impact on NO_2^- production at varying sizes (Figure 1). Despite the varying media across studies (e.g. sediment, activated sludge, and soil; Dai et al., 2020; Fang et al., 2024; Li et al., 2020; Seeley et al., 2020; Yin et al., 2023), the size of the MPs could be responsible for the inconsistencies in these studies.

Taken together, the treatment of specific MPs regulates the strength of NO_2^- production and consumption. However, there is no clear information regarding which specific process in the NO_2^- cycling is impacted by MPs. For instance, the observed NO_2^- concentrations in the MP treatments were higher than that in the control, but we do not know exactly which source process was promoted by the MPs (NH_3 oxidation or dissimilatory NO_3^- reduction). Similarly, the consumption of NO_2^- depends on which NO_2^--consuming process is either promoted or impeded by the MPs. In light of these aspects, we offer an in-depth discussion using NO_2^- dual isotopes.

3.2 Isotopic evidence for the impact of MPs on nitrite production

This study first reports the impact of MPs on the isotopic signatures of NO_2^- (Figure 3) and analyzes the NO_2^- transformation pathways accordingly (Figures 3, 4). The impact of MPs on the source of NO_2^- was mainly analyzed on day 18 in our experiments, as NO_2^- was continuously produced, although there may also have been a simultaneous partial consumption of NO_2^-. As for the subsequent NO_2^- consumption stage, the regulation of the NO_2^- pool by the NO_2^- consumption process was mainly considered, and therefore the analysis of the source process in this stage was not made here. Before an analysis of the specific source process of NO_2^-, one basic framework that needs to be stated is that compared with $\delta^{15}N_{NO2}$, $\delta^{18}O_{NO2}$ has the advantage of distinguishing signals from two potential sources (NH_3 oxidation and dissimilatory NO_3^- reduction) of NO_2^-, since the $\delta^{18}O_{NO2}$ values produced by these two processes are on opposite sides of the expected equilibrium value ($\delta^{18}O_{NO2,\ eq}$, when O isotope exchange equilibrium is reached between NO_2^- and ambient H_2O) (Buchwald and Casciotti, 2013; Casciotti, 2016a, 2016b; Chen et al., 2021; Chen et al., 2022a; Chen and Chen, 2022; Figure 4). Specifically, NO_2^- from dissimilatory NO_3^- reduction has a higher $\delta^{18}O_{NO2}$ than that from NH_3 oxidation, with the latter being lower than the equilibrium value (Buchwald and Casciotti, 2013; Casciotti, 2016a, 2016b; Chen et al., 2021; Chen et al., 2022a; Chen and Chen, 2022; Figure 4). Thus, although we did not measure the isotopes of NO_3^- and NH_4^+, the major source of NO_2^- could be inferred from

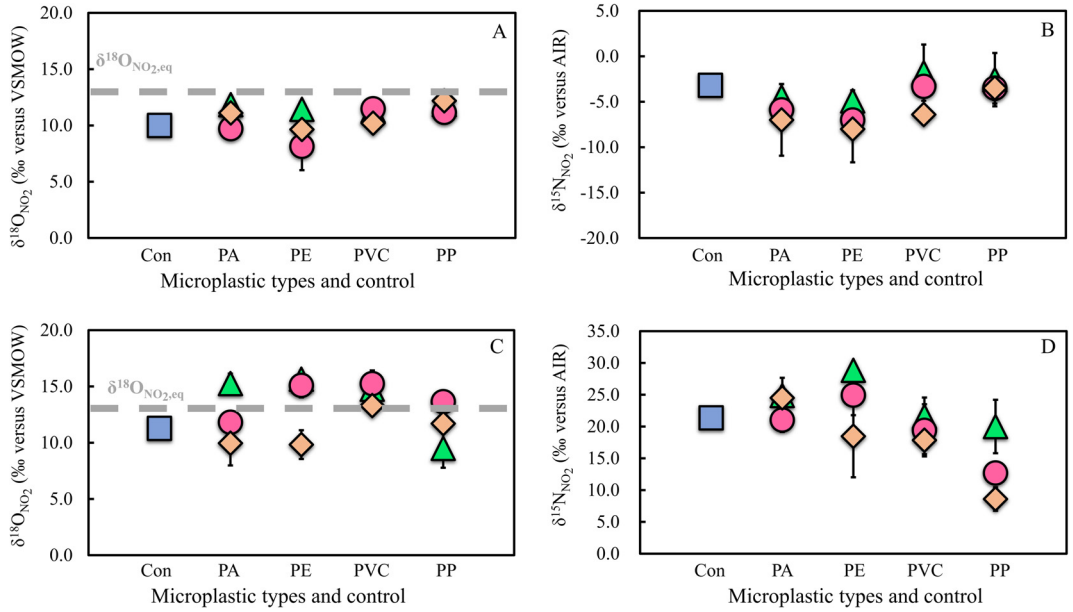

FIGURE 3
The impact of MPs on nitrite isotope dynamics. **(A, B)** represent changes in $\delta^{15}N_{NO2}$ and $\delta^{18}O_{NO2}$ during the nitrite accumulation stage in the control and MP treatments, respectively, while **(C, D)** are changes during the nitrite consumption stage. The blue square represents the control. The grey lines in **(A, C)** represent the $\delta^{18}O_{NO2,\ eq}$ and the black lines are the error bars.

the measured $\delta^{18}O_{NO2}$ compared to the $\delta^{18}O_{NO2,\ eq}$. Using the equations from Buchwald and Casciotti, 2013, along with the measured temperature in the overlying water for each treatment and the assumed $\delta^{18}O$ value of the H_2O (0‰, Buchwald and Casciotti, 2013), we then estimated the $\delta^{18}O_{NO2,\ eq}$ in our experimental system to be 13.2 ± 0.1‰. During the NO_2^- accumulation stage, both the MPs and the control treatments were relatively close to each other in terms of $\delta^{18}O_{NO2}$ and all were slightly lower than the $\delta^{18}O_{NO2,\ eq}$ (Figure 3A and Figure 4), implying that the NO_2^- accumulation in all treatments was mainly contributed by NH_3 oxidation (Buchwald and Casciotti, 2013; Casciotti, 2016a, 2016b; Chen et al., 2021, 2022; Chen and Chen, 2022; Figure 4).

Thus, based on isotopic evidence, the higher or lower accumulation of NO_2^- in the MP treatment compared to the control may indicate that the polymer type and size of the MPs either promoted or impeded NH_3 oxidation, a specific NO_2^- source process. For instance, in the case of PE-0.02 mm, the accumulated NO_2^- was lower than that of the control (Figure 1C). Furthermore, given that its $\delta^{18}O_{NO2}$ was lower than the equilibrium value (Figures 3A, 4), this may imply that this treatment may have impeded NH_3 oxidation, leading to a lower accumulated concentration of NO_2^-. However, the assessment regarding this impediment impact should be viewed with caution. This is because, although we focus on the role of NO_2^- source processes in regulating the NO_2^- pool at this stage, NO_2^- consumption processes may also be operating simultaneously. These consumption processes may alter $\delta^{18}O_{NO2}$, which, in turn, may affect the assessment of the impact of MPs on NO_2^- production. Therefore, in conjunction with the analysis of $\delta^{15}N_{NO2}$, we provide a comprehensive analysis of this aspect below.

3.3 Retention vs loss of nitrogen in the environment—the role of MPs

The fate of NO_2^- determines whether N is lost or retained in the environment, influencing greenhouse gas N_2O production and the environmental N budget. However, the impact of MP pollution on NO_2^- consumption pathways remains unclear (Fang et al., 2024; Green et al., 2016; Hope et al., 2020; Seeley et al., 2020). To investigate this, we used NO_2^- dual isotope data (Figures 3A, B), similar to analyzing the effect of MPs on NO_2^- source processes. Before proceeding, we must also clarify the effects of NO_2^- oxidation, denitrification (dissimilatory NO_2^- reduction), and anammox on NO_2^- dual isotopes to better assess the specific processes impacted by MPs. NO_2^- oxidation, either driven by NO_2^--oxidizing bacteria (Buchwald and Casciotti, 2010; Casciotti, 2009) or anammox bacteria (Brunner et al., 2013; Kobayashi et al., 2019), is expected to decrease both $\delta^{15}N_{NO2}$ (Figure 3C) and $\delta^{18}O_{NO2}$ (Figure 3D) (Brunner et al., 2013; Buchwald and Casciotti, 2010; Casciotti, 2009; Kobayashi et al., 2019). Denitrification is discussed here as dissimilatory NO_2^- reduction, since dissimilatory NO_3^- reduction, although also part of the denitrification, is a process that acts as the source of NO_2^-. Dissimilatory NO_2^- reduction will result in an increase in $\delta^{18}O_{NO2}$ (Figure 3C) and $\delta^{15}N_{NO2}$ (Figure 3D) (Martin and Casciotti, 2016). Similarly, the operation of anammox will also result in an increase in $\delta^{15}N_{NO2}$ during NO_2^- reduction to N_2

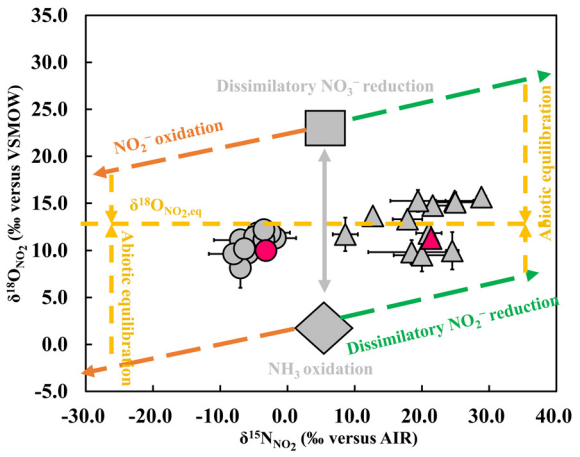

FIGURE 4
Schematic description of biogeochemical processes affecting nitrite isotopes. Possible sources of NO_2^- include dissimilatory NO_3^- reduction (grey square) and NH_3 oxidation (grey diamond). The isotopic values for these two sources are not specific and are shown a range based on previous reports (41, 43, 45, 46). Possible NO_2^- consumption processes in our experiment include NO_2^- oxidation (orange dashed line), dissimilatory NO_2^- reduction (green dashed line), and anammox (not shown). Given that the O isotope effect for the reduction of NO_2^- to N_2 in the anammox process is not yet known, its effect on NO_2^- dual isotopes is not shown in the figure. The horizontal yellow dashed line represents $\delta^{18}O_{NO2,\ eq}$, while the vertical yellow dashed and grey lines represent abiotic equilibrium processes and source mixing processes (41-46). The circle and triangle colored in red represent the CON and the black lines are error bars.

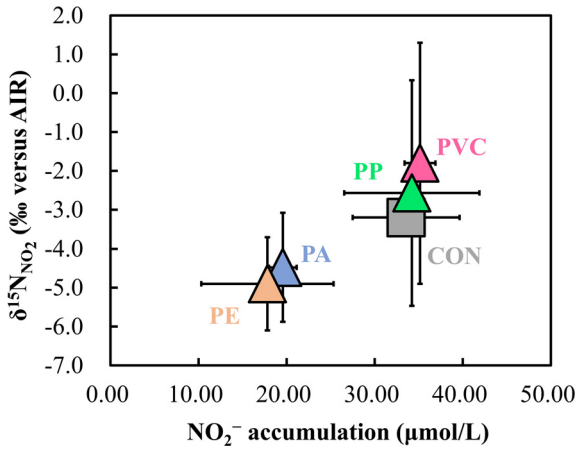

FIGURE 5
Relationship between nitrite concentration and $\delta^{15}N_{NO2}$ during the nitrite accumulation stage. The various colored circles represent the MPs of different polymer types with the smallest size, while the black lines represent error bars.

(Brunner et al., 2013; Kobayashi et al., 2019), but its effect on $\delta^{18}O_{NO2}$ remains unclear (Casciotti, 2016b; Kobayashi et al., 2019).

In light of the effects of these consumption processes on NO_2^- concentration and isotopes, we herein first reevaluate the reliability of the above discussion of the impacts of MPs on NO_2^- production, focusing on treatments with lower NO_2^- accumulation compared to the control. Some treatments, such as PA-0.02 mm, PE-0.02 mm, and PE-0.1 mm, had lower NO_2^- concentrations compared to the control (Figure 1C), implying that NO_2^- production may have been impeded. However, the relationship between NO_2^- accumulation and $\delta^{15}N_{NO2}$ revealed a deviation in the PA-0.02 mm and PE-0.02 mm treatments (Figure 5), indicating enhanced NO_2^- oxidation, which can simultaneously decrease both NO_2^- concentration and $\delta^{15}N_{NO2}$ (Brunner et al., 2013; Buchwald and Casciotti, 2010; Casciotti, 2009; Kobayashi et al., 2019). A similar effect was observed in the PE-0.1 mm treatment (Supplementary Figure S3). However, as the MP size increased, the impact of NO_2^- oxidation on the NO_2^- pool became limited (Supplementary Figure S4), likely due to the maximal NO_2^-yield (Figure 2), making the NO_2^- oxidation insufficient to significantly reduce NO_2^-accumulation. Consequently, the lower NO_2^- concentrations in small-sized MP treatments may not be solely due to reduced NO_2^- production, but rather the promotion of NO_2^-oxidation.

It is important to note that stronger NO_2^- oxidation in these treatments may confound $\delta^{18}O$ -based evaluations of NO_2^- source processes, as this process would lower $\delta^{18}O_{NO2}$ (Brunner et al., 2013; Buchwald and Casciotti, 2010; Casciotti, 2009; Kobayashi et al., 2019), potentially masking the contribution of dissimilatory NO_3^- reduction to NO_2^- production (Figure 4). But here, we focus mainly on whether the lower NO_2^- concentrations in these MP treatments relative to the control were due to source processes being impeded, regardless of the specific source process. Obviously, the above analysis is a good example to show the ability of natural abundance stable isotopes in addressing the impact of MPs on the N cycle.

Furthermore, during the NO_2^- consumption stage, the $\delta^{15}N_{NO2}$ was higher in the MP and the control treatments than in the previous stage (Figure 3D). This shows that the NO_2^- in some MP treatments, including the control, was consumed primarily through dissimilatory NO_2^- reduction or anammox (Figure 4). However, some MP treatments showed outliers in $\delta^{15}N_{NO2}$ relative to the control (Figure 3D), meaning that there may have been variations in the pathway or strength of NO_2^- consumption. The presence of these outliers further supports size as an important factor in considering the impact of MPs on the N cycle. By analyzing these outliers, we can capture valuable information about the impact of MPs on the biogeochemical cycling of NO_2^-. Accordingly, we performed a discussion of the relationship between NO_2^- concentration (residual), degree of NO_2^- consumption, $\delta^{15}N_{NO2}$ of residual NO_2^-, and $\delta^{15}N_{NO2}$ variation in the MPs and control treatments during the NO_2^- consumption stage (Figure 6, Supplementary Figures S5-S7). Among these, the degree of NO_2^- consumption and $\delta^{15}N_{NO2}$ variation represent the quantity of NO_2^- consumed and the impact of the NO_2^--consuming process on $\delta^{15}N_{NO2}$ over the period of 18–25 days, respectively.

The first case is enhanced NO_2^- oxidation (arrow 1 in Figure 6). The $\delta^{15}N_{NO2}$ decreased with increasing NO_2^- consumption in the PP treatment of different sizes (Figure 6, Supplementary Figures S5-S7). In particular, for the PP treatment at 1 mm, the NO_2^- consumption was higher than that of the control, yet $\delta^{15}N_{NO2}$ was lower (Figure 6). The low $\delta^{15}N_{NO2}$ signal during NO_2^- consumption could either be due to a low $\delta^{15}N_{NO2}$ during the

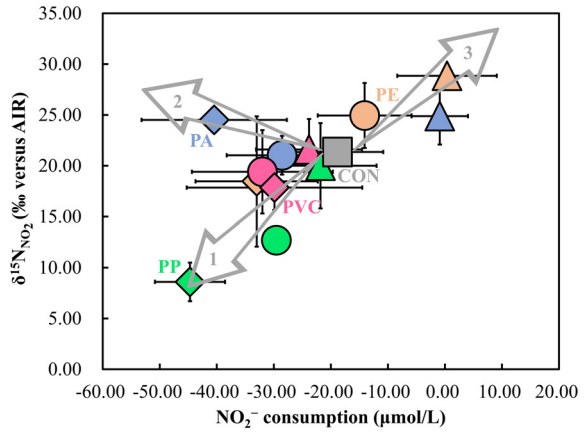

FIGURE 6
Relationship between the $\delta^{15}N_{NO2}$ and degree of NO_2^- consumption. Differences in NO_2^- concentrations on day 18 and day 25 in the experiment were used to create this figure. The numbers 1, 2, and 3 in the figure represent the three pathways of nitrite consumption, respectively. The different numerical labels on the arrows indicate the impact of MPs on NO_2^- fate and the black lines are error bars. The triangles, circles, and diamonds represent the smallest, medium and largest sizes of MPs, respectively.

previous NO_2^- accumulation stage compared to the control or a smaller increase in $\delta^{15}N_{NO2}$ during NO_2^- consumption. The first possibility can be excluded, as $\delta^{15}N_{NO2}$ values were consistent across treatments and the control during NO_2^- accumulation (Figure 3B). Therefore, the second possibility must be considered. As shown by the relationship between NO_2^- consumption and $\delta^{15}N_{NO2}$variation, the $\delta^{15}N_{NO2}$ increase in the PP treatment was smaller than in the control as NO_2^- consumption increased (Supplementary Figures S5-S7). This suggests a contribution of dissimilatory NO_2^- reduction or anammox (Brunner et al., 2013; Martin and Casciotti, 2016; Kobayashi et al., 2019), but the limited increase implies these processes were weaker than in the control. If these processes were weaker, NO_2^- consumption would be lower, which contradicts the higher NO_2^- consumption in the PP treatments (Figure 6, Supplementary Figures S5-S7). Thus, another process must be consuming NO_2^- and limiting $\delta^{15}N_{NO2}$ increase. We propose that NO_2^- oxidation played a more significant role in NO_2^- consumption in the PP-0.1 mm and PP-1 mm treatments (Figure 6, Supplementary Figure S6, and Supplementary Figure S7), as it can both consume $NO_2^-$and reduce $\delta^{15}N_{NO2}$ (Figure 4, Brunner et al., 2013; Buchwald and Casciotti, 2010; Casciotti, 2009; Kobayashi et al., 2019). This suggests that in environments polluted by these MPs, NO_2^- may be retained as bioavailable N, potentially reducing N_2O greenhouse gas production.

The second scenario is enhanced dissimilatory NO_2^- reduction or anammox (arrow 2 in Figure 6). The higher $\delta^{15}N_{NO2}$ values and NO_2^- consumption in some MP treatments, especially PA-1mm, imply a stronger operation of dissimilatory NO_2^- reduction or anammox (Figure 4, Brunner et al., 2013; Martin and Casciotti, 2016; Kobayashi et al., 2019). This is further supported by the observation that in the PA-1mm treatment, the increase in $\delta^{15}N_{NO2}$ during NO_2^- consumption was greater than in the control (Supplementary Figure S6 and Supplementary Figure S7). Unlike the previous scenario, this indicates that more NO_2^- is being lost from the environment as gas (N_2O or N_2) in this scenario, suggesting that the production of the greenhouse gas N_2O may be enhanced.

The final scenario may involve an enhanced dissimilatory NO_3^- reduction and dissimilatory NO_2^- reduction (or anammox) (arrow 3 in Figure 6). This scenario is distinct because, although NO_2^- consumption was limited, there was an increase in $\delta^{15}N_{NO2}$ compared to the control (PE-0.02 mm, PE-0.1 mm, PA-0.02 mm, Figure 6, Supplementary Figure S5, and Supplementary Figure S6). The increase in $\delta^{15}N_{NO2}$ suggests that dissimilatory NO_2^- reduction or anammox are the primary processes responsible for NO_2^- consumption (Figure 4; Brunner et al., 2013; Martin and Casciotti, 2016; Kobayashi et al., 2019). However, since NO_2^- consumption was not significant, we propose that dissimilatory NO_3^- reduction, the first step of denitrification, may also be regulating the NO_2^- pool. This could offset NO_2^- consumption, and the $\delta^{18}O_{NO2}$ analysis supports this hypothesis. The $\delta^{18}O_{NO2}$ values of these MP treatments were all higher than the control and equilibrium values (Figure 3C), indicating a contribution from dissimilatory NO_3^- reduction (Figure 4). Consequently, the imbalance between the source and consumption of NO_2^- in this scenario likely led to insufficient NO_2^- consumption coupled with increased $\delta^{15}N_{NO2}$. When considered in terms of NO_2^- consumption pathways, this also reveals a promotion of dissimilatory NO_2^- reduction or anammox in these MP treatments compared to the control. Without the isotope data, such low consumption of NO_2^- in these MP treatments might have been considered to be an inhibition of the dissimilatory NO_2^- reduction or anammox by these MPs relative to the control. Thus, this is once again a prime example of the value of natural abundance stable isotopes in identifying the real impact of MPs on the N cycle.

Overall, the isotopic evidence clearly indicates that the consumption pathways of NO_2^- vary depending on the polymer type and size of the MPs, which plays a crucial role in determining whether the production of the greenhouse gas N_2O in the environment increases or decreases. This suggest that MPs may contribute to local variations in greenhouse gas emissions, potentially altering greenhouse gas inventories in affected regions (Li et al., 2022; Ren et al., 2020; Su et al., 2022; Wang et al., 2024). These findings underscore the importance of considering MPs as an emerging environmental factor in greenhouse gas management. Future studies should aim to explore the long-term effects of MPs on N transformations and their cumulative impact under various environmental stressors, thereby improving the accuracy of greenhouse gas emission inventories and informing more effective mitigation strategies.

4 Conclusions

Conclusively, our study presents the first picture of the impact of MPs with distinct polymer types and sizes on specific N cycle

transformation processes based on the natural abundance of N and O isotope ratios of NO_2^-. This offers a new perspective for a more comprehensive and accurate evaluation of the impact of sediment exposure to MP pollution on the biogeochemical cycling of NO_2^- in aquatic ecosystems, which has profound implications for reconciling the balance of the environmental N budget and assessing greenhouse gas production in the context of increasing MP pollution. It is worth noting that while our study aims to provide a new paradigm for the study of the impact of MPs on the N cycle, the reasons behind the unique regulation of the N cycle by MPs with distinct polymer types and sizes remain to be further addressed.

Data availability statement

The original contributions presented in the study are included in the article/Supplementary Material. Further inquiries can be directed to the corresponding author.

Author contributions

YC: Conceptualization, Data curation, Formal analysis, Funding acquisition, Investigation, Methodology, Writing – original draft, Writing – review & editing. XZ: Data curation, Formal analysis, Investigation, Methodology, Writing – original draft. YY: Investigation, Methodology, Validation, Writing – original draft. MC: Data curation, Formal analysis, Resources, Writing – review & editing.

Funding

The author(s) declare financial support was received for the research, authorship, and/or publication of this article. This work was supported by National Natural Science Foundation of China (42306055), Natural Science Foundation of Jiangsu Province (BK20230695), and Open-end Funds of Jiangsu Key Laboratory of Marine Biotechnology, Jiangsu Ocean University (HS2022001).

Acknowledgments

We thank Minfang Zheng and Mengya Chen for their help with the isotopic analysis. We also thank Xueting Chen for her assistance in sample processing.

Conflict of interest

The authors declare that the research was conducted in the absence of any commercial or financial relationships that could be construed as a potential conflict of interest.

Generative AI statement

The author(s) declare that no Generative AI was used in the creation of this manuscript.

Publisher's note

Supplementary material

The Supplementary Material for this article can be found online at: https://www.frontiersin.org/articles/10.3389/fmars.2025.1518631/full#supplementary-material

References

Amaral-Zettler, L. A., Zettler, E. R., and Mincer, T. J. (2020). Ecology of the plastisphere. *Nat. Rev. Microbiol.* 18, 139–151. doi: 10.1038/s41579-019-0308-0

Azizi, S. M. M., Hai, F. I., Lu, W., Al-Mamun, A., and Dhar, B. R. (2021). A review of mechanisms underlying the impacts of (nano) MPs on anaerobicdigestion. *Bioresource Technol.* 329, 124894. doi: 10.1016/j.biortech.2021.124894

Baysal, A., Saygin, H., and Ustabasi, G. S. (2020). MPs occurrences in sediments collected from marmara sea-istanbul, Turkey. *Bull. Environ. Contam. Toxicol.* 105, 522–529. doi: 10.1007/s00128-020-02993-9

Brunner, B., Contrerasa, S., Lehmann, M. F., Matantseva, O., Rollog, M., Kalvelage, T., et al. (2013). Nitrogen isotope effects induced by anammox bacteria. *Proc. Natl. Acad. Sci. U.S.A.* 110, 18994–18999. doi: 10.1073/pnas.1310488110

Buchwald, C., and Casciotti, K. L. (2010). Oxygen isotopic fractionation and exchange during bacterial nitrite oxidation. *Limnol. Oceanogr.* 55, 1064–1074. doi: 10.4319/lo.2010.55.3.1064

Buchwald, C., and Casciotti, K. L. (2013). Isotopic ratios of nitrite as tracers of the sources and age of oceanic nitrite. *Nat. Geosci.* 6, 308–313. doi: 10.1038/ngeo1745

Casciotti, K. L. (2009). Inverse kinetic isotope fractionation during bacterial nitrite oxidation. *Geochim. Cosmochim. Acta* 73, 2061–2076. doi: 10.1016/j.gca.2008.12.022

Casciotti, K. L. (2016a). Nitrogen and oxygen isotopic studies of the marine nitrogen cycle. *Annu. Rev. Mar. Sci.* 8, 379–407. doi: 10.1146/annurev-marine-010213-135052

Casciotti, K. L. (2016b). Nitrite isotopes as tracers of marine N cycle processes. *Philos. Trans. R. Soc A* 374, 20150295. doi: 10.1098/rsta.2015.0295

Casciotti, K. L., Böhlke, J. K., McIlvin, M. R., Mroczkowski, S. J., and Hannon, J. E. (2007). Oxygen isotopes in nitrite: analysis, calibration, and equilibration. *Anal. Chem.* 79, 2427–2436. doi: 10.1021/ac061598h

Chen, Y. J., Bardhan, P., Zhao, X. F., Zheng, M. F., Qiu, Y. S., and Chen, M. (2021). Nitrite cycle indicated by dual isotopes in the northern South China Sea. *J. Geophys. Res. Biogeosciences* 126, e2020JG006129. doi: 10.1029/2020JG006129

Chen, Y. J., and Chen, M. (2022). Nitrite cycling in warming Arctic and Subarctic waters. *Geophys. Res. Lett.* 49, e2021GL096947. doi: 10.1029/2021GL096947

Chen, Y. J., Chen, M., Chen, J. X., Fan, L. F., Zheng, M. F., and Qiu, Y. S. (2022a). Dual isotopes of nitrite in the Amundsen Sea in summer. *Sci. Total Environ.* 843, 157055. doi: 10.1016/j.scitotenv.2022.157055

Chen, C., Pan, J., Xiao, S., Wang, J., Gong, X., Yin, G., et al. (2022b). Microplastics alter nitrous oxide production and pathways through affecting microbiome in estuarine sediments. *Water Res.* 221, 118733. doi: 10.1016/j.watres.2022.118733

Cluzard, M., Kazmiruk, T. N., Kazmiruk, V. D., and Bendell, L. I. (2015). Intertidal concentrations of MPs and their influence on ammonium cycling as related to the shellfish industry. Arch. *Environ. Contam. Toxicol.* 69, 310–319. doi: 10.1007/s00244-015-0156-5

Dai, H. H., Gao, J., Wang, Z., Zhao, Y., and Zhang, D. (2020). Behavior of nitrogen, phosphorus and antibiotic resistance genes under polyvinyl chloride MPs pressures in an aerobic granular sludge system. *J. Clean. Prod.* 256, 120402. doi: 10.1016/j.jclepro.2020.120402

de Souza MaChado, A. A., Lau, C. W., Kloas, W., Bergmann, J., Bachelier, J. B., Faltin, E., et al. (2019). MPs can change soil properties and affect plant performance. *Environ. Sci. Technol.* 53, 6044–6052. doi: 10.1021/acs.est.9b01339

Fang, C., Yang, Y., Zhang, S., He, Y., Pan, S., Zhou, L., et al. (2024). Unveiling the impact of MPs with distinct polymer types and concentrations on tidal sediment microbiome and nitrogen cycling. *J. Hazard. Mater.* 472, 134387. doi: 10.1016/j.jhazmat.2024.134387

Granger, J., Boshers, D. S., Böhlke, J. K., Yu, D., Chen, N., and Tobias, C. R. (2020). The influence of sample matrix on the accuracy of nitrite N and O isotope ratio analyses with the azide method. *Rapid Commun. Mass Spectrom.* 34, e8569. doi: 10.1002/rcm.v34.1

Green, D. S., Boots, B., Sigwart, J., Jiang, S., and Rocha, C. (2016). Effects of conventional and biodegradable MPs on a marine ecosystem engineer (Arenicola marina) and sediment nutrient cycling. *Environ. pollut.* 208, 426–434. doi: 10.1016/j.envpol.2015.10.010

Greenfield, L. M., Graf, M., Rengaraj, S., Bargiela, R., Williams, G., and Golyshin, P. N. (2022). Field response of N_2O emissions, microbial communities, soil biochemical processes and winter barley growth to the addition of conventional and biodegradable MPs. *Agric. Ecosyst. Environ.* 336, 108023. doi: 10.1016/j.agee.2022.108023

Hartmann, N. B. (2019). Are we speaking the same language? Recommendations for a definition and categorization framework for plastic debris. *Environ. Sci. Technol.* 53, 1039–1047. doi: 10.1021/acs.est.8b05297

Hope, J. A., Coco, G., and Thrush, S. F. (2020). Effects of polyester microfibers on microphytobenthos and sediment-dwelling infauna. *Environ. Sci. Technol.* 54, 7970–7982. doi: 10.1021/acs.est.0c00514

Hu, H., Bourbonnais, A., Larkum, J., Bange, H. W., and Altabet, M. A. (2016). Nitrogen cycling in shallow low-oxygen coastal waters off Peru from nitrite and nitrate nitrogen and oxygen isotopes. *Biogeosciences* 13, 1453–1468. doi: 10.5194/bg-13-1453-2016

Hu, X. J., Gu, H. D., Sun, X. X., Wang, Y. B., Liu, J. J., Yu, Z. H., et al. (2023). Distinct influence of conventional and biodegradable MPs on microbe-driving nitrogen cycling processes in soils and plastispheres as evaluated by metagenomic analysis. *J. Hazard. Mater.* 451, 131097. doi: 10.1016/j.jhazmat.2023.131097

Ikenoue, T., Nakajima, R., Osafune, S., Siswanto, E., and Honda, M. C. (2024). Vertical flux of microplastics in the deep subtropical Pacific Ocean: moored sediment-trap observations within the Kuroshio Extension recirculation gyre. *Environ. Sci. Technol.* 58, 16121–16130. doi: 10.1021/acs.est.4c02212

Ikenoue, T., Yamada, M., Ishii, N., Kudo, N., Shirotani, Y., Ishida, Y., et al. (2022). Cesium-137 and $^{137}Cs/^{133}Cs$ atom ratios in marine zooplankton off the east coast of Japan during 2012–2020 following the Fukushima Dai-ichi nuclear power plant accident. *Environ. pollut.* 311, 119962. doi: 10.1016/j.envpol.2022.119962

Kobayashi, K., Fukushima, K., Onishi, Y., Nishina, K., Makabe, A., and Yano, M. (2021). Influence of $\delta^{18}O$ of water on measurements of $\delta^{18}O$ of nitrite and nitrate. *Rapid Commun. Mass Spectrom.* 35, e89799. doi: 10.1002/rcm.v35.2

Kobayashi, K., Makabe, A., Yano, M., Oshiki, M., Kindaichi, T., Casciotti, K. L., et al. (2019). Dual nitrogen and oxygen isotope fractionation during anaerobic ammonium oxidation by anammox bacteria. *ISME J.* 13, 2426–2436. doi: 10.1038/s41396-019-0440-x

Lebreton, L. C. M., van der Zwet, J., Damsteeg, J.-W., Slat, B., Andrady, A., and Reisser, J. (2017). River plastic emissions to the world's oceans. *Nat. Commun.* 8, 1–10. doi: 10.1038/ncomms15611

Lee, J., Jeong, S., Long, C., and Chandran, K. (2022). Size dependent impacts of a model microplastic on nitrification induced by interaction with nitrifying bacteria. *J. Hazard Mater.* 424, 127363. doi: 10.1016/j.jhazmat.2021.127363

Li, H., and Liu, L. (2022). Short-term effects of polyethene and polypropylene MPs on soil phosphorus and nitrogen availability. *Chemosphere* 291, 132984. doi: 10.1016/j.chemosphere.2021.132984

Li, L., Song, K., Yeerken, S., Geng, S. X., Liu, D., and Dai, Z. L. (2020). Effect evaluation of MPs on activated sludge nitrification and denitrification. *Sci. Total Environ.* 707, 135953. doi: 10.1016/j.scitotenv.2019.135953

Li, X., Yao, S., Wang, Z., Jiang, X., Song, Y., and Chang, S. X. (2022). Polyethylene MPs and biochar interactively affect the global warming potential of soil greenhouse gas emissions. *Environ. pollut.* 315, 120433. doi: 10.1016/j.envpol.2022.120433

Lyu, L., Wu, Y., Chen, Y. J., Li, J., Chen, Y., and Wang, L. (2024). Synergetic effects of chlorinated paraffins and microplastics on microbial communities and nitrogen cycling in deep-sea cold seep sediments. *J. Hazard. Mater.* 480, 135760. doi: 10.1016/j.jhazmat.2024.135760

Martin, T. S., and Casciotti, K. L. (2016). Nitrogen and oxygen isotopic fractionation during microbial nitrite reduction. *Limnol. Oceanogr.* 61, 1134–1143. doi: 10.1002/lno.10278

Mato, Y., Isobe, T., Takada, H., Kanehiro, H., Ohtake, C., and Kaminuma, T. (2001). Plastic resin pellets as a transport medium for toxic chemicals in the marine environment. *Environ. Sci. Technol.* 35, 318–324. doi: 10.1021/es0010498

McIlvin, M. R., and Altabet, M. A. (2005). Chemical conversion of nitrate and nitrite to nitrous oxide for nitrogen and oxygen isotopic analysis in freshwater and seawater. *Anal. Chem.* 77, 5589–5595. doi: 10.1021/ac050528s

Oberbeckmann, S., Löder, M. G. J., and Labrenz, M. (2015). Marine MPs associated biofilms-a review. *Environ. Chem.* 12, 551–562. doi: 10.1071/EN15069

Pinnell, L. J., and Turner, J. W. (2019). Shotgun metagenomics reveals the benthic microbial community response to plastic and bioplastic in a coastal marine environment. *Front. Microbiol.* 10, 1–13. doi: 10.3389/fmicb.2019.01252

Ren, X., Tang, J., Liu, X., and Liu, Q. (2020). Effects of MPs on greenhouse gas emissions and the microbial community in fertilized soil. *Environ. pollut.* 256, 113347. doi: 10.1016/j.envpol.2019.113347

Rillig, M. C., Hoffmann, M., Lehmann, A., Liang, Y., Lück, M., and Augustin, J. (2021). MPs fibers affect dynamics and intensity of CO_2 and N_2O fluxes from soil differently. *Microplast. Nanoplast.* 1, 3. doi: 10.1186/s43591-021-00004-0

Riveros, G., Urrutia, H., Araya, J., Zagal, E., and Schoebitz, M. (2022). MPs pollution on the soil and its consequences on the nitrogen cycle: a review. *Environ. Sci. pollut. Res.* 29, 7997–8011. doi: 10.1007/s11356-021-17681-2

Seeley, M. E., Song, B., Passie, R., and Hale, R. C. (2020). MPs affect sedimentary microbial communities and nitrogen cycling. *Nat. Commun.* 11, 2372. doi: 10.1038/s41467-020-16235-3

Shen, M., Song, B., Zhou, C., Almatrafi, E., Hu, T., Zeng, G., et al. (2022). Recent advances in impacts of microplastics on nitrogen cycling in the environment: A review. *Sci. Total Environ.* 815, 152740. doi: 10.1016/j.scitotenv.2021.152740

Song, K., Wang, R., Yang, G., Xie, S., Chen, Y., and Yang, F. (2023). Pollution concerns in mariculture water and cultured economical bivalves: Occurrence of MPs under different aquaculture modes. *J. Clean. Prod.* 406, 136913. doi: 10.1016/j.jclepro.2023.136913

Strickland, J. D. H., and Parsons, T. R. (1972). A practical handbook of seawater analysis. *Bull. Fish. Res. Board Canada* 167, 1–310. doi: 10.1002/iroh.19700550118

Su, X., Yang, L., Yang, K., Tang, Y., Wen, T., and Wang, Y. (2022). Estuarine plastisphere as an overlooked source of N_2O production. *Nat. Commun.* 13, 3884. doi: 10.1038/s41467-022-31584-x

Sun, X., Tao, R., Xu, D., Qu, M., Zheng, M., Zhang, M., et al. (2023). Role of polyamide microplastic in altering microbial consortium and carbon and nitrogen cycles in a simulated agricultural soil microcosm. *Chemosphere* 312, 137155. doi: 10.1016/j.chemosphere.2022.137155

Vo, H. C., and Pham, M. H. (2021). Ecotoxicological effects of MPs onaquatic organisms: a review. *Environ. Sci. pollut. Res.* 28, 44716–44725. doi: 10.1007/s11356-021-14982-4

Wan, Y., Wu, C., Xue, Q., and Hui, X. (2018). Effects of plastic contamination on water evaporation and desiccation cracking in soil. *Sci. Total Environ.* 654, 576–582. doi: 10.1016/j.scitotenv.2018.11.123

Wang, W., Ge, J., and Yu, X. (2020). Bioavailability and toxicity of MPs to fish species: a review. *Ecotoxicol. Environ. Saf.* 189, 109913. doi: 10.1016/j.ecoenv.2019.109913

Wang, W. F., Zhang, Z. Y., Gao, J., and Wu, H. T. (2024). The impacts of MPs on the cycling of carbon and nitrogen in terrestrial soil ecosystems: Progress and prospects. *Sci. Total Environ.* 915, 169977. doi: 10.1016/j.scitotenv.2024.169977

Wang, P. Y., Zhao, Z.-Y., Xiong, X.-B., Wang, N., Zhou, R., and Zhang, Z.-M. (2023). MPs affect soil bacterial community assembly more by their shapes rather than the concentrations. *Water Res.* 24, 120581. doi: 10.1016/j.watres.2023.120581

Yin, M. Y., Wang, H., Wu, Y., Wang, X., and Wang, J. (2023). Effects of MPs on nitrogen and phosphorus cycles and microbial communities in sediments. *Environ. pollut.* 318, 120852. doi: 10.1016/j.envpol.2022.120852

Yu, Y., Li, X., Feng, Z., Xiao, M., Ge, T., and Li, Y. (2022). Polyethylene MPs alter the microbial functional gene abundances and increase nitrous oxide emissions from paddy soils. *J. Hazard. Mater.* 432, 128721. doi: 10.1016/j.jhazmat.2022.128721

Zhang, X., Ward, B. B., and Sigman, D. M. (2020). Global nitrogen cycle: critical enzymes, organisms, and processes for nitrogen budgets and dynamics. *Chem. Rev.* 120, 5308–5351. doi: 10.1021/acs.chemrev.9b00613

Zhang, G. S., Zhang, F. X., and Li, X. T. (2019). Effects of polyester microfibers on soil physical properties: perception from a field and a pot experiment. *Sci. Total Environ.* 670, 1–7. doi: 10.1016/j.scitotenv.2019.03.149

Zhu, F., Yan, Y. Y., Doyle, E., Zhu, C. Y., Jin, X., and Chen, Z. H. (2022). MPs altered soil microbiome and nitrogen cycling: the role of phthalate plasticizer. *J. Hazard. Mater.* 427, 127944. doi: 10.1016/j.jhazmat.2021.127944